HHS Public Access

Author manuscript

Biochimie. Author manuscript; available in PMC 2020 May 01.

Published in final edited form as:

Biochimie. 2019 May ; 160: 113–121. doi:10.1016/j.biochi.2019.02.015.

Grem2 Mediates Podocyte Apoptosis in High Glucose Milieu

Hongxiu Wen[1,2], **Vinod Kumar**[2], **Abheepsa Mishra**[2], **Su Song**[2], **Rukhsana Aslam**[2], **Ali Hussain**[2], **Haichao Wang**[2,3], **Xiaogang Zhou**[1], **Xiaoming He**[1], **Guisheng Wu**[1], **Huairong Luo**[1], **Xiqian Lan**[1,2,*], **Ashwani Malhotra**[2], **Pravin C Singhal**[2,*]

[1]Key Laboratory for Aging and Regenerative Medicine, School of Pharmacy, Southwest Medical University, Luzhou, Sichuan, China

[2]Feinstein Institute for Medical Research and Donald and Barbara Zucker School of Medicine at Hofstra/Northwell, Manhasset, NY, United States

[3]Department of Emergency Medicine, North Shore University Hospital, Manhasset, NY, United States

Abstract

Background: Increased DAN protein (Grem1, Grem2, Grem3, Cerberus, NBL1, SOST, and USAG1) levels are often associated with severe disease-states in adult kidneys. Grem1, SOST, and USAG1 have been demonstrated to be upregulated and play a critical role in the progression of diabetic nephropathy (DN); however, the expression and the role of other DAN family members in DN have not been reported yet. In this study, we investigated the expression and the role of Grem2 in the development of renal lesions in mice with type 2 DN.

Methods: Fourteen-week-old BTBR$^{ob/ob}$ (a mouse model of type 2 diabetes mellitus) and control (BTBR, wild type) mice were evaluated for renal functional and structural biomarkers. Urine was collected for protein content assay, and renal tissues were harvested for molecular analysis with real-time PCR, Western blotting, and immunohistochemistry. *In vitro* studies, human podocytes were transfected with Grem2 plasmid and were evaluated for apoptosis (morphologic assay and Western blotting). To evaluate the Grem2-mediated downstream signaling, the phosphorylation status of Smad2/3 and Smad1/5/8 was assessed. To establish a causal relationship, the effect of SIS3 (an inhibitor for Samd2/3) and BMP-7 (an agonist for Smad1/5/8) was evaluated on Germ2-induced podocyte apoptosis.

Results: BTBR$^{ob/ob}$ mice showed elevated urinary protein levels. Renal tissues of BTBR$^{ob/ob}$ mice showed an increased expression of Grem2; both glomerular and tubular cells displayed enhanced Grem2 expression. *In vitro* studies, high glucose increased Grem2 expression in cultured

[*]**Corresponding author:** psinghal@northwell.edu, xlan@swmu.edu.cn.

Author Contribution

Study design: X.L., H.Wang, P.C.S.;

Experiment conduction: H.Wen, V.K., A.M., S.S., R.A., A.H, X.H., X.L.;

Data analysis: X.L., H.Wang, P.C.S., A.M.;

Manuscript writing and revision: H.Wen, X.L., H.Wang, V.K., X.Z., G.W., H.L., P.C.S.

human podocytes, whereas, Grem2 silencing partially protected podocyte from high glucose-induced apoptosis. Overexpression of Grem2 in podocytes not only increased Bax/Bcl2 expression ratio but also promoted podocyte apoptosis; moreover, an overexpression of Grem2 increased the phosphorylation of Smad2/3 and decreased the phosphorylation of Smad1/5/8; furthermore, SIS3 and BMP-7 attenuated Grem2-induced podocyte apoptosis.

Conclusions: High glucose increases Grem2 expression in kidney cells. Grem2 mediates podocyte apoptosis through Smads.

Keywords

Grem2; podocyte; apoptosis; high glucose milieu

1. Introduction

Diabetic nephropathy (DN) is one of the major complications of diabetes mellitus, manifesting in the form of progressive proteinuria, a decline in glomerular filtration rate (GFR), hypertension, and a higher risk of cardiovascular morbidity and mortality. It is the largest single cause of end-stage renal disease (ESRD) in many developed countries including the United States [1]. In China, glomerulonephritis was used to be considered as the leading cause of ESRD [2, 3]; a recent study has revealed that at least in large cities such as Beijing and Shanghai, the percentage of patients with chronic kidney disease related to diabetes exceeded the percentage of patients with chronic kidney disease related to glomerulonephritis [4]. Since pathogenesis of the development and progression of DN is not fully understood, its management is predominantly dependent on controlling the blood sugar levels. However, current therapeutic approaches are not effective in controlling the development and progression of DN; therefore, the majority of patients still progress to ESRD, creating a socioeconomic burden in the society [5]. This necessitates the identification and validation of unexplored pathogenic molecules contributing to DN, and the efforts to develop relevant therapeutic strategies to prevent or delay DN progression.

The DAN family represents a collection of Bone morphogenetic protein (BMP) antagonists including seven members: Grem1 (Gremlin-1), Grem2 (Gremlin-2 or PRDC), Grem3 (Coco), Cerberus, NBL1 (Dan), SOST, and USAG1 (Wise) [6]. These members are highly expressed during embryonic development, and occupy important roles in the limb bud formation and digitation, the kidney formation and morphogenesis, and the left-right axis specification [7–11]. In adults, however, increased DAN protein levels are often associated with severe disease-states, including pulmonary and renal fibrosis and cancer [6]. For instance, Grem1 is not expressed in normal human adult kidneys, but is abundantly expressed in those kidneys with DN and possibly contributing to renal dysfunction [12–15]. Animal studies have demonstrated that renal tubular overexpression of Grem1 aggravates renal damage in DN in transgenic mice [16]. On the other hand, allelic depletion of grem1 attenuates diabetic kidney disease [17].

In addition to Grem1, SOST and USAG1, are also up-regulated in DN, but down-regulation of their expression slows down the progression of renal lesions [18–21]. The role of other DAN family members, including Grem2, Grem3, NBL1, and Cerberus, in the development

and progression has not been investigated yet. Since Grem2 shows high homology with Grem1 in the amino acid sequence [6], we reasoned that it might play a similar role as Grem1 in the pathogenesis of DN. In addition, Grem2 has been reported to suppress the BMP-2-induced osteogenesis [22], suggesting that it may also suppress the role of BMPs in the kidney. In this study, we investigated the expression and the role of the remaining DAN family members with a focus on Grem2 in the development of DN in type 2 diabetes mouse model.

2. Materials and Methods

2.1. Animal experiments

All animal experiments complied with Institutional Animal Care and Use Committee (IACUC)-approved protocols. BTBR$^{ob/ob}$ mice, a type 2 diabetic mouse model, and control mice were purchased from Jackson Laboratory (Bar Harbor, ME, USA), and were housed within the rodent holding facilities in the Feinstein Institute for Medical Research (Northwell Health) in Manhasset, New York. It is under temperature, light and humidity control. Adequate food, water, and bedding were provided. Two male and female of each group mice (14 weeks old) were used in this study. Mice were sacrificed by carbon dioxide asphyxiation, and death was confirmed by cervical dislocation.

2.2. Culture of human podocytes

Human podocytes were cultured as previously reported [23–24]. Briefly, immortalized human podocytes proliferated in the growth medium containing RPMI 1640 supplemented with 10% fetal bovine serum, 1 X penicillin- streptomycin, 1 mM L-glutamine, and 1 X insulin, transferrin, and selenium (ITS) (Invitrogen, Grand Island, NY) at permissive temperature (33°C). When the cells reached about 80% confluence, they were transferred to 37°C for differentiation in a medium without ITS for 7 days.

2.3. Grem2 overexpression

Human podocytes (5×10^5) were cultured in 60 mm dish. After differentiation for 7 days, the cells were transfected with 1 mg pCMV3-Grem2 plasmid (Sino Biological, Wayne, PA) by using the Effectene Transfection Reagent (Qiagen, Germantown, MD) following the manufacturer's instruction.

2.4. Real-time PCR

Total RNA was isolated from mouse kidney tissue using Trizol reagent (Invitrogen). Five micrograms of total RNA were reverse transcribed using the first-strand synthesis system (Invitrogen). Real-time PCR was performed in a Prism 7900HT sequence-detection system (Applied Biosystems, Foster City, CA, USA). Relative mRNA levels were determined and standardized with a GAPDH internal control using a comparative CT method. Sequences of primers for the targeting genes are listed in Table 1.

2.5. Western blot analysis

Western blotting was performed using established methodology [23–24]. Briefly, cells were washed with PBS and lysed in RIPA buffer (1 X PBS, pH7.4, 0.1% SDS, 1% NP-40, 0.5% sodium deoxycholate, 1.0 mM sodium orthovanadate, 10 ml of protease inhibitor cocktail (100 x, Calbiochem) per 1 ml of buffer, and 100 mg/ml PMSF). Proteins (20–30 mg) were separated by 12% SDS-polyacrylamide gel electrophoresis (PAGE) and then transferred on an Immuno-Blot polyvinylidene fluoride (PVDF) membrane (Bio-Rad, Hercules, CA). After blocking in PBS/Tween (0.1%) with 5% nonfat milk, the membrane was incubated with primary antibodies overnight at 4°C followed by horseradish peroxidase-conjugated secondary antibodies (Santa Cruz Biotechnology, 1:5000) and then developed using Enhanced Chemiluminescent (ECL) solution (Pierce). Primary antibodies used were rabbit anti-Grem2 (Novus Biologicals, NBP1–31150, 1:1000), rabbit anti-Bax (Santa Cruz Biotechnology, sc-526, 1:1000), goat anti-Bcl2 (Santa Cruz Biotechnology, sc-492-g, 1:1000), rabbit anti-P-Smad2/3 (Abcam, ab63399, 1:1000), rabbit anti-P-Smad1/5/8 (Millipore Sigma, AB3848-I, 1:1000), and mouse anti-actin (Santa Cruz Biotechnology, sc-8432, 1:3000). For protein expression quantification, the films were scanned with a CanonScan 9950F scanner, and the acquired images were then analyzed using the public domain NIH image program (http://rsb.info.nih.gov/nih-image/).

2.6. Immunofluorescent microscopy

Immunofluorescent microscopy was performed as discussed in our previous publications [23, 24]. Briefly, the kidneys were perfused *in situ* and then fixed with fresh 4% PFA and stored at −80°C. Subsequently, paraffin sections (4 μm) were prepared and de-paraffinized in xylene and re-hydrated through graded concentrations of alcohol. Epitope retrieval was carried out by heating the samples at 98 °C for 2 h in Retrieveall-1 (Sign et Laboratories, Inc.). Subsequently, cooled samples were permeabilized with 0.3% Triton X-100 for 10 min, and were blocked with 2% BSA in 0.1% Triton X-100 for 1h at room temperature. Sections were then incubated with primary antibodies overnight at 4°C, followed by Alexa Fluo r secondary antibodies (Invitrogen, 1:800), donkey anti-rabbit IgG Alexa Fluor 568 or donkey anti-goat lgG Alexa Fluor 488, for 1 hour at room temperature. Primary antibodies included rabbit anti-Grem2 (Novus Biologicals, NBP1–31150, 1:100), goat anti-nephrin (R&D system, 1:100). All antibodies were diluted in 0.1% Triton X-100, 2% BSA in PBS. Cells were then counterstained with Hoechst33342 (Sigma-Aldrich) to identify nuclei. Morphological changes were visualized and captured with a ZEISS microscope (Carl Zeiss MicoImaging GmbH, Jena, Germany) equipped with a digital imaging system.

2.7. Apoptotic cell determination

We detected apoptotic cells by using Hoechst33342 staining as described in our previous publications [23, 25]. Briefly, after appropriate treatment, the culture media was removed, and the cells were fixed with 4% PFA for 15 min. After that, Hoechst 33342 (10 μg/ml) was added. After 10 min, cell images were taken with a ZEISS microscope (Carl Zeiss MicoImaging GmbH, Jena, Germany) equipped with a digital imaging system. Apoptotic cells were identified as nucleus condensed and fragmented.

2.8. Statistical analyses

Data were presented as means ± standard deviation (SD) unless otherwise noted. All experiments were repeated at least three times with duplicate or triplicate samples in each assay. All data were evaluated statistically by the analysis of variance (ANOVA), followed by Newman-Keuls multiple comparison tests using software (Prism 4.0, GraphPad Software). In the case of single mean comparison, data were analyzed by t-test. P values < 0.05 were considered as statistically significant.

3. Results

3.1. Hyperglycemia associated with podocyte apoptosis in mice

Compared with age-matched wild type mice, BTBR$^{ob/ob}$ mice (14 weeks old) showed overt manifestations of diabetes, such as an increased body weight (control, 25 ± 3 g vs. BTBR$^{ob/ob}$, 38± 5 g) and higher blood glucose concentrations (control, 130 ± 20 mg/dl vs. BTBR$^{ob/ob}$, 585± 80 mg/dl). We also monitored the blood glucose concentrations of both wild type and BTBR$^{ob/ob}$ mice from 8 to 14 weeks old, and found that they didn't significantly change (data not shown). The BTBR $^{ob/ob}$ mice also showed a higher urinary albumin-to-creatinine ratio and a greater percentage of apoptotic cells in their glomeruli (Figure 1); these findings suggest that the kidney function was affected by hyperglycemia in BTBR$^{ob/ob}$ mice.

3.2. Grem2 is upregulated in high glucose milieu

We performed real-time PCR to investigate the expression of DAN family members in the kidneys of adult wild type and BTBR$^{ob/ob}$ mice. Results showed that the expression of Grem1, Grem2, and SOST were all up-regulated in BTBR$^{ob/ob}$ mice when compared with age-matched wild type controls (Figure 2); while USAG1 expression was not altered overtly. As to the other DAN family members (Cer1, Nbl1, and Grem3), their expressions were barely detectable (data not shown). Since the role of Grem2 on DN has not been reported yet, we focused on it in the present study.

To confirm the expression of Grem2 in the kidneys of BTBR$^{ob/ob}$ mice, we performed Western blotting to detect renal tissue protein expression. The results showed that renal tissue expression of Grem2 in BTBR$^{ob/ob}$ mice was higher than that in control wild type mice (Figure 3AB). We also performed immunofluorescent studies on kidney paraffin sections, and found that in control mice, the Grem2 expression was barely presented, while in BTBR$^{ob/ob}$ mice its expression was significantly higher (Figure 3CD). We also found that the expression of Grem2 was co-localized with Nephrin (a molecular marker of podocyte phenotype), indicating that Grem2 expression was increased in podocytes of BTBR$^{ob/ob}$ mice (Figure 4).

To examine the role of high glucose on Grem2 expression *in vitro*, we treated human podocytes with normal (5 mM) and high glucose (30 mM) for 48 h, and then collected cellular lysate for Western blotting. Results showed that the expression Grem2 in high glucose media was higher than that in normal glucose media (Figure 5). Combined, these results demonstrated that Grem2 expression could be upregulated by high glucose.

3.3. Overexpression of Grem2 increases podocyte apoptosis

Grem1 has been reported to induce podocyte apoptosis [26]. To test whether Grem2 has a similar function, we overexpressed Grem2 in human podocytes, and then counted the cells with apoptotic phenotype. We found that podocytes overexpressing Grem2 showed enhanced apoptosis when compared with control podocytes (Figure 6AB). To further confirm this observation, we collected the cellular lysates and performed Western blotting for the expression of apoptosis-related molecules. Results showed that overexpression of Grem2 increased the expression of Bax (a pro-apoptotic molecule) and decreased the expression of Bcl2 (an anti-apoptotic molecule) (Figure 6C-F). These results indicate that the expression of Grem2 carries a potential to enhance podocyte apoptosis.

3.4. Suppressing Grem2 attenuates high glucose-induced podocyte apoptosis

Although it has been shown that high glucose can induce podocyte apoptosis [27–29], it was previously unknown whether Grem2 plays an important role in this process. To test this possibility, we silenced Grem2 expression by using siRNA and then treated them with high glucose. Heochst33342 staining results showed that high glucose caused podocyte apoptosis while silencing Grem2 expression decreased the number of apoptotic cells in the high-glucose milieu (Figure 7).

3.5. Grem2 mediates high glucose-induced apoptosis through Smads

Grem1 has been reported to activate Smad2/3 and suppress the activation of Smad1/5/8. To test whether Grem2 has a similar function, we overexpressed Grem2 in human podocytes and performed Western blotting to determine the phosphorylation of Smad2/3 and Smad1/5/8. Results showed that Grem2 overexpression significantly increased the expression of p-Smad2/3 but decreased the expression of Smad1/5/8 (Figure 8).

To detect the role of Smad2/3 and Smad1/5/8 in Grem2-mediated apoptosis, we transfected pCMV3-Grem2 plasmid to human podocytes and then added either SIS3, an inhibitor specific for Smad2/3 phosphorylation, or recombinant BMP-7, an agonist for Samd1/5/8. After 48 h, we evaluated the number of apoptotic cells. We found that overexpression of Grem2 significantly increased the number of apoptotic cells, while the addition of either SIS3 or BMP-7 protected induction of apoptosis in Grem2 expressing podocytes (Figure 9); these findings suggest that inhibition of Smad3 or activation of Smad1/5/8 prevented Grem2-induced podocyte apoptosis.

4. Discussion

As a secreted member of cysteine knot superfamily, Grem2 belongs to a family of bone morphogenetic proteins (BMPs) antagonists. It interacts with these BMPs, in particular with BMPs −2, −4, and −7, blocking their bindings to their specific receptors, and regulating downstream related processes [6, 22]. The amino acid sequence of Grem2 shows high homology with that of Grem1, indicating that they may play similar roles in kidney fibrosis. In this study, we found that Grem2 expression in podocyte is significantly increased in high glucose milieu, and that genetic enhancing or silencing Grem2 expression divergently affected high glucose-induced apoptosis. Also, we found that overexpression of Grem2 in

podocyte activates Smad2/3 but suppress Smad1/5/8, while inhibiting Smad2/3 or activating Smad1/5/8 could attenuate Grem2-induced apoptosis. Taken together, these results demonstrate that Grem2 contribute, at least partially, to the development and progression of podocyte injury in DN. To our knowledge, this is the first report to show the role of Grem2 in kidney disease.

The Grem2 expression has been reported to be highest in the brain but much lower in kidney and lung [30]; consistent with this, we also found that Grem2 expression was barely detected in the kidney of wild type mice. However, we found its overt expression in the kidney of diabetic mice. Additionally, high glucose-induced Grem2 expression in cultured human podocytes. These results indicate that Grem2 expression can be induced by high glucose milieu in adult kidney. Whether high glucose also increases its expression in other organs, such as the brain, still need to be determined.

TGF-β and BMPs (especially BMP-2, −4, and −7) are the key members in the TGF-β superfamily, playing important but diverse roles in chronic kidney diseases (CKDs). They share similar downstream Smad signaling pathways but counter-regulate each other to maintain the balance of their biological activities. TGF-β acts as an essential mediator in kidney diseases through the phosphorylation of fibrosis-associated Smad2/3; whereas BMPs exhibits its anti-fibrotic and anti-inflammatory properties through the phosphorylation of reno-protection-associated Smad1/5/8 [31]. In our study, we found that Grem2 participates in both pathways, because overexpression of Grem2 significantly increased the phosphorylation of Smad2/3 but decreased the phosphorylation of Smad1/5/8. We also noted that inhibition of Smad2/3 with SIS3 or activation of Smad1/5/8 with BMP-7 attenuated Grem2-induced podocyte apoptosis. These results demonstrate that both Smad2/3 and Smad1/5/8 are involved in the Grem2-associated renal cell injury. Interestingly, SIS3 could prevent Germ2-induced apoptosis completely, whereas, BMP-7 could prevent it only partially, suggesting that Smad2/3 may be the involved major pathway in Grem2-induced podocyte apoptosis.

The protein peptide sequences of matured Grem1 and Grem2 show high homology [6], suggesting their similar properties with a similar role in the development and progression of DN. In this study, we found that Grem2 induces podocyte apoptosis mainly through activation of Smad2/3, and this is akin to the role played by Grem1, which has been reported to promote podocyte apoptosis through TGF-β/Smad2/3 signaling pathway [26]. It is reported that tubular overexpression of Grem1 contributes to renal damage susceptibility in mice [16, 32]; while allelic depletion of grem1 prevents diabetic kidney disease [17]. Considering the high homology between Grem1 and Grem2, we speculate that overexpression of Grem2 will also contribute to renal damage susceptibility in mice, and suppression of its expression will attenuate diabetic kidney disease. To validate this hypothesis, it will be interesting to carry out *in vivo* studies with modulation of Grem2 expression (both up and down) in future.

In addition to Grem1 and Grem2, among the DAN family members, SOST and USAG1, have also been reported to play important roles in DN [18–21]. Consistent with these reports, we also found that the mRNA expression of SOST increased in the kidney of

diabetic mice. However, we did not found any significant difference in USAG1 expression between the wild type and diabetic mice. The expression of other DAN family members (Cer1, Nbl1, and Grem3) was barely detectable in kidney cells, suggesting that they may not be contributing to the development and progression of DN.

In the present study, we investigated the role of Grem2 on kidney disease. We found that Grem2 expression was significantly induced by high glucose in both *in vivo* and *in vitro* studies. Overexpression of Grem2 in podocytes increased apoptosis; while silencing of Grem2 expression partially attenuated high glucose-induced podocyte apoptosis. Grem2 overexpression increased the phosphorylation of Smad2/3 but decreased that of Smad1/5/8 in podocytes. Inhibition of Smad2/3 with its inhibitor, SIS3 or activation of Smad1/5/8 with BMP-7 protected podocyte from Grem2-induced apoptosis. These results suggest that in high glucose milieu, Grem2 promotes podocyte apoptosis through the activation of Smad2/3 and suppression of Smad1/5/8. Out study demonstrates an important role of Grem2 in the development of kidney disease, and highlights new potential target for the prevention and therapy of DN.

5. Conclusions

High glucose increases Grem2 expression in kidney cells. Grem2 mediates podocyte apoptosis through Smads.

Acknowledgment

This work was supported by the Luzhou Science and Technology Bureau grant (2018LZXNYD-ZK12, Luzhou, Sichuan, China); the NIH grants R01DK098074 and RO1DK118017 (to P.C.S); the National Institute of General Medical Sciences grants (R01GM063075 and 1R41GM123858 to H.Wang); the National Center of Complementary and Alternative Medicine grant (R01AT005076 to H.Wang).

Reference

1. John S. Complication in diabetic nephropathy. Diabetes Metab Syndr 2016; 10 (4): 247–249. [PubMed: 27389078]
2. Barsoum RS. Chronic kidney disease in the developing world. N Engl J Med 2006; 354: 997–999. [PubMed: 16525136]
3. Wang H, Zhang L, Lv J. Prevention of the progression of chronic kidney disease: Practice in China. Kidney Int Suppl 2005; 67: S63–67.
4. Zhang L, Long J, Jiang W, Shi Y, He X, Zhou Z, Li Y, Yeung RO, Wang J, Matsushita K, Coresh J, Zhao MH, Wang H. Trends in chronic kidney disease in China. N Engl J Med 2016; 375: 905–906. [PubMed: 27579659]
5. Gheith O, Farouk N, Nampoory N, Halim MA, Al-Otaibi T. Diabetic kidney disease: world wide difference of prevalence and risk factors. J Nephropharmacol 2015; 5 (1): 49–56. [PubMed: 28197499]
6. Nolan K, Thompson TB. The DAN family: modulators of TGF-β signaling and beyond. Protein Sci 2014; 23: 999–1012. [PubMed: 24810382]
7. Michos O, Panman L, Vintersten K, Beier K, Zeller R, Zúñiga A. Gremlin-mediated BMP antagonism induces the epithelial-mesenchymal feedback signaling controlling metanephric kidney and limb organogenesis. Development 2004; 131: 3401–3410. [PubMed: 15201225]
8. Michos O, Gonçalves A, Lopez-Rios J, Tiecke E, N aillat F, Beier K, Galli A, Vainio S, Zeller R. Reduction of BMP4 activity by Gremlin 1 enables ureteric bud outgrowth and GDNF/WNT11

feedback signalling during kidney branching morphogenesis. Development 2007; 134: 2397–2405. [PubMed: 17522159]

9. Khokha MK, Hsu D, Brunet LJ, Dionne MS, Harland RM. Gremlin is the BMP antagonist required for maintenance of Shh and Fgf signals during limb patterning. Nat Genet 2003; 34: 303–307. [PubMed: 12808456]
10. Zúñiga A, Haramis AP, McMahon AP, Zeller R. Signal relay by BMP antagonism controls the SHH/FGF4 feedback loop in vertebrate limb buds. Nature 1999; 401: 598–602. [PubMed: 10524628]
11. Marques S, Borges AC, Silva AC, Freitas S, Cordenonsi M, Belo JA. The activity of the Nodal antagonist Cerl-2 in the mouse node is required for correct L/R body axis. Genes Dev 2004; 18: 2342–2347. [PubMed: 15466485]
12. Dolan V, Murphy M, Sadlier D, Lappin D, Doran P, Godson C, Martin F, O'Meara Y, Schmid H, Henger A, Kretzler M, Droguett A, Mezzano S, Brady HR. Expression of gremlin, a bone morphogenetic protein antagonist, in human diabetic nephropathy. Am J Kidney Dis 2005;45 (6): 1034–1039. [PubMed: 15957132]
13. Walsh DW, Roxburgh SA, McGettigan P, Berthier CC, Higgins DG, Kretzler M, Cohen CD, Mezzano S, Brazil DP, Martin F. Co-regulation of Gremlin and Notch signaling in diabetic nephropathy. Biochim Biophys Acta 2008;1782 (1): 10–21. [PubMed: 17980714]
14. Murphy M, Crean J, Brazil DP, Sadlier D, Martin F, Godson C. Regulation and consequences of differential gene expression in diabetic kidney disease. Biochem Soc Trans 2008; 36 (Pt 5): 941–945. [PubMed: 18793165]
15. Lappin DW, McMahon R, Murphy M, Brady HR. Gremlin: an example of the re-emergence of developmental programmes in diabetic nephropathy. Nephrol Dial Transplant 2002;17 Suppl 9: 65–67. [PubMed: 12386293]
16. Marchant V, Droguett A, Valderrama G, Burgos ME, Carpio D, Kerr B, Ruiz-Ortega M, Egido J, Mezzano S. Tubular overexpression of Gremlin in transgenic mice aggravates renal damage in diabetic nephropathy. Am J Physiol Renal Physiol 2015; 309 (6): F559–568. [PubMed: 26155842]
17. Roxburgh SA, Kattla JJ, Curran SP, O'Meara YM, Pollock CA, Goldschmeding R, Godson C, Martin F, Brazil DP. Allelic depletion of grem1 attenuates diabetic kidney disease. Diabetes 2009; 58 (7): 1641–1650. [PubMed: 19401426]
18. Thomsen LH, Fog-Tonnesen M, Nielsen Fink L, Norlin J, García de Vinuesa A, Hansen TK, de Heer E, Ten Dijke P, Rosendahl A. Disparate phospho-Smad2 levels in advanced type 2 diabetes patients with diabetic nephropathy and early experimental db/db mouse model. Ren Fail 2017; 39 (1): 629–642. [PubMed: 28805484]
19. Pena MJ, Heinzel A, Heinze G, Alkhalaf A, Bakker SJ, Nguyen TQ, Goldschmeding R, Bilo HJ, Perco P, Mayer B, de Zeeuw D, Lambers Heerspink HJ. A panel of novel biomarkers representing different disease pathways improves prediction of renal function decline in type 2 diabetes. PLoS One 2015; 10 (5): e0120995. [PubMed: 25973922]
20. Lv W, Guan L, Zhang Y, Yu S, Cao B, Ji Y. Sclerostin as a new key factor in vascular calcification in chronic kidney disease stages 3 and 4. Int Urol Nephrol 2016; 48 (12): 2043–2050. [PubMed: 27465794]
21. Tanaka M, Asada M, Higashi AY, Nakamura J, Oguchi A, Tomita M, Yamada S, Asada N, Takase M, Okuda T, Kawachi H, Economides AN, Robertson E, Takahashi S, Sakurai T, Goldschmeding R, Muso E, Fukatsu A, Kita T, Yanagita M. Loss of the BMP antagonist USAG-1 ameliorates disease in a mouse model of the progressive hereditary kidney disease Alport syndrome. J Clin Invest 2010; 120 (3): 768–777. [PubMed: 20197625]
22. Wang CL, Xiao F, Wang CD, Zhu JF, Shen C, Zuo B, Wang H, Li, Wang XY, Feng WJ, Li ZK, Hu GL, Zhang X, Chen XD. Gremlin2 Suppression Increases the BMP-2-Induced Osteogenesis of Human Bone Marrow-Derived Mesenchymal Stem Cells Via the BMP-2/Smad/Runx2 Signaling Pathway. J Cell Biochem 2017; 118 (2): 286–297. [PubMed: 27335248]
23. Lan X, Lederman R, Eng JM, Shoshtari SS, Saleem MA, Malhotra A, Singhal PC. Nicotine Induces Podocyte Apoptosis through Increasing Oxidative Stress. PLoS One 2016; 11 (12): e0167071. [PubMed: 27907022]

24. Lan X, Wen H, Cheng K, Plagov A, Marashi Shoshtari SS, Malhotra A, Singhal PC. Hedgehog pathway plays a vital role in HIV-induced epithelial-mesenchymal transition of podocyte. Exp Cell Res 2017; 352 (2): 193–201. [PubMed: 28159470]

25. Vashistha H, Husain M, Kumar D, Singhal PC. Tubular cell HIV-1 gp120 expression induces caspase 8 activation and apoptosis. Ren Fail 2009; 31: 303–312.

26. Li G, Li Y, Liu S, Shi Y, Chi Y, Liu G, Shan T. Gremlin aggravates hyperglycemia-induced podocyte injury by a TGFβ/smad dependent signaling pathway. J Cell Biochem 2013; 114 (9): 2101–2113. [PubMed: 23553804]

27. Li R, Dong W, Zhang S, Yang H, Zhang L, Ye Z, Zhao X, Zhang H, Li Z, Xu L, Liu S, Shi W, Liang X. Septin 7 mediates high glucose-induced podocyte apoptosis. Biochem Biophys Res Commun 2018; 506 (3): 522–528. [PubMed: 30361092]

28. Jin Y, Liu S, Ma Q, Xiao D, Chen L. Berberine enhances the AMPK activation and autophagy and mitigates high glucose-induced apoptosis of mouse podocytes. Eur J Pharmacol 2017; 794: 106–114 [PubMed: 27887947]

29. Khazim K, Gorin Y, Cavaglieri RC, Abboud HE, Fanti P. The antioxidant silybin prevents high glucose-induced oxidative stress and podocyte injury in vitro and in vivo. Am J Physiol Renal Physiol 2013; 305 (5): F691–700. [PubMed: 23804455]

30. Church RH, Ali I, Tate M, Lavin D, Krishnakumar A, Kok HM, Hombrebueno JR, Dunne PD, Bingham V, Goldschmeding R, Martin F, Brazil DP. Gremlin1 plays a key role in kidney development and renal fibrosis. Am J Physiol Renal Physiol 2017; 312 (6): F1141–F1157. [PubMed: 28100499]

31. Meng XM, Chung AC, Lan HY. Role of the TGF-β/BMP-7/Smad pathways in renal diseases. Clin Sci (Lond) 2013; 124 (4): 243–254. [PubMed: 23126427]

32. Droguett A, Krall P, Burgos ME, Valderrama G, Carpio D, Ardiles L, Rodriguez-Diez R, Kerr B, Walz K, Ruiz-Ortega M, Egido J, Mezzano S. Tubular overexpression of gremlin induces renal damage susceptibility in mice. PLoS One 2014; 9 (7): e101879. [PubMed: 25036148]

Highlights

1. Grem2 expression in podocytes is upregulated in high glucose milieu.
2. Overexpression of Grem2 promotes podocyte apoptosis.
3. Grem2 suppression attenuates high glucose-induced podocyte apoptosis.
4. Grem2 mediates high glucose-induced podocyte apoptosis through Smads.

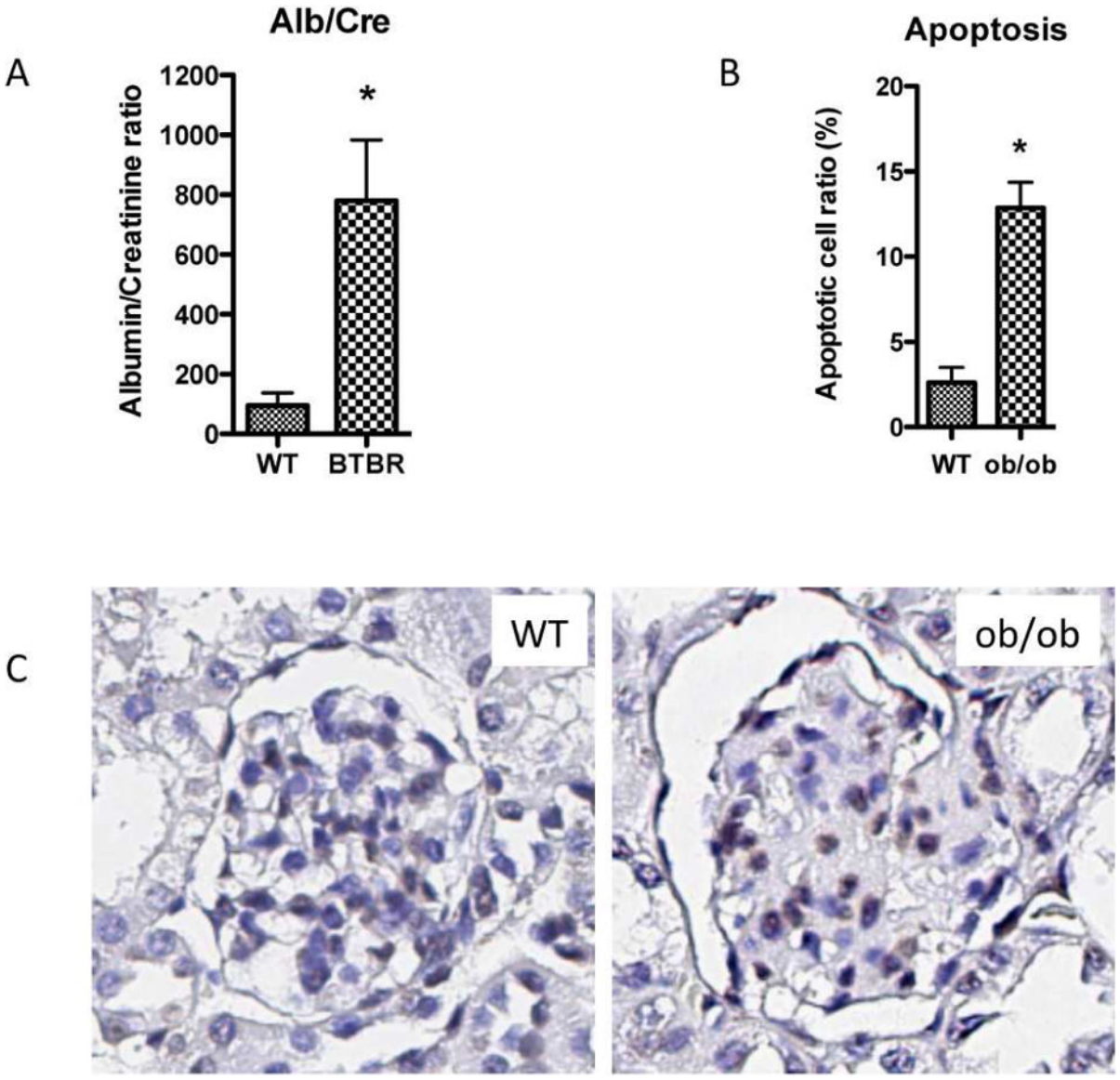

Figure 1. Hyperglycemia causes severe kidney injury.

Fourteen-week-old BTBR wild type (WT) and diabetic (ob/ob) mice were used to investigate the kidney injuries caused by hyperglycemia. Urine samples were collected to determine the albumin-to-creatinine ratio (A). The mice were sacrificed, and the kidney samples were collected for TUNEL staining to detect the apoptotic cells in the glomeruli (B-C). The results (mean ± SD) represent 10 randomly selected regions (B), and the representative figures are displayed (C). * $P < 0.05$ when compared with wild type (WT).

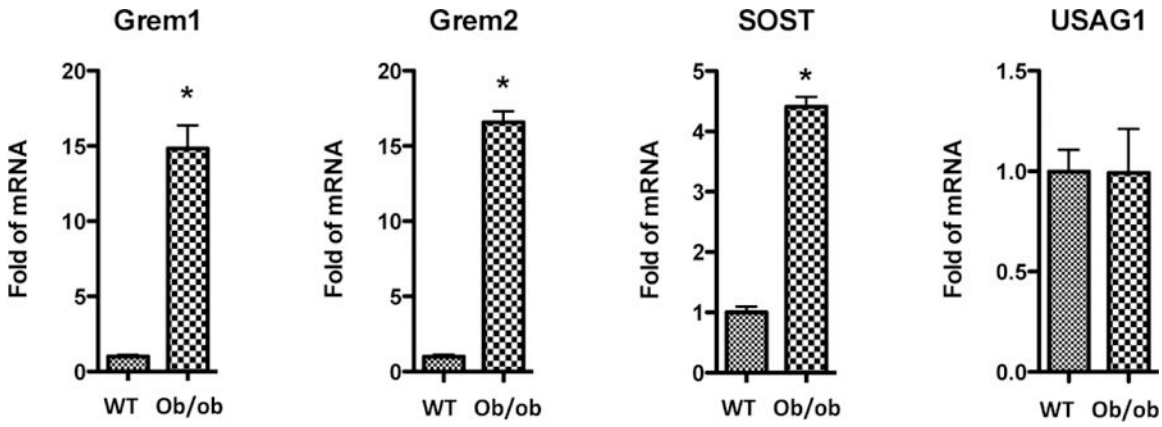

Figure 2. Expression of DAN family members in mouse kidneys.

RNA samples were collected from the kidneys of 14-week-old BTBR wild type (WT) and diabetic (ob/ob) mice, and real-time PCR was performed to compare the expression changes of the genes for DAN family members. * $P < 0.05$ when compared with wild type (WT).

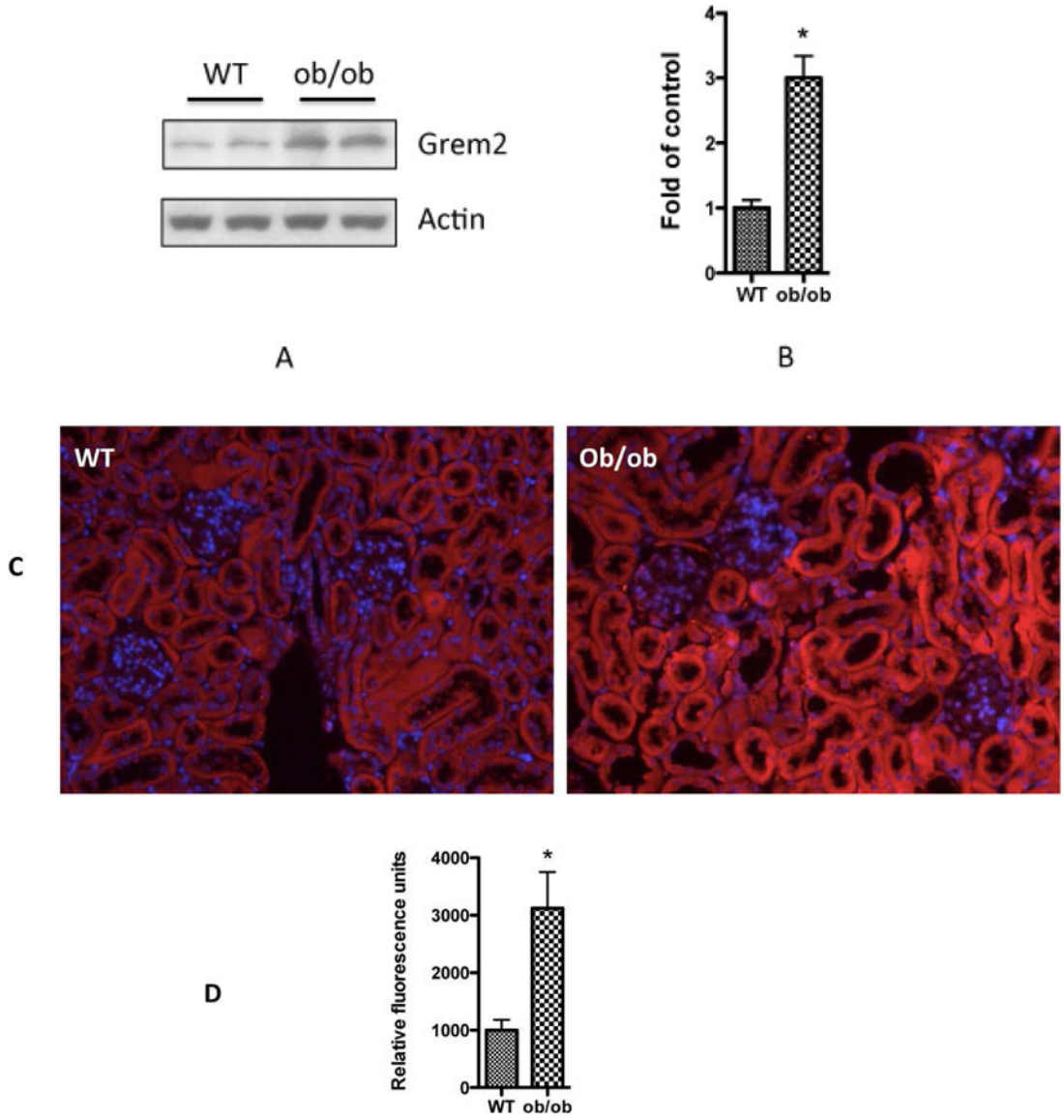

Figure 3. Expression of Grem2 in mouse kidneys.

Fourteen-week-old BTBR wild type (WT) and diabetic (ob/ob) mice were used to investigate the expression of Grem2 in the kidney. The kidneys were homogenized, and the tissue lysates were subjected to Western blotting to detect the expression of Grem2 (A-B). Representative gels are displayed (A), and the protein bands were scanned, and the acquired images were analyzed using the public domain NIH image program for data quantification (B). Expression of Grem2 was normalized to β-actin, and the results (mean ± SD) represent three independent samples. Paraffin sections were prepared for immune-fluorescence staining to detect the Grem2 expression in the kidneys (C-D). Representative fluoromicrographs are displayed (C). The average fluorescence intensity was measured per region of interest (ROI) for Grem2, and the results (mean ± SD) represent 10 randomly selected regions (D). * $P < 0.05$ when compared with the wild type control mice.

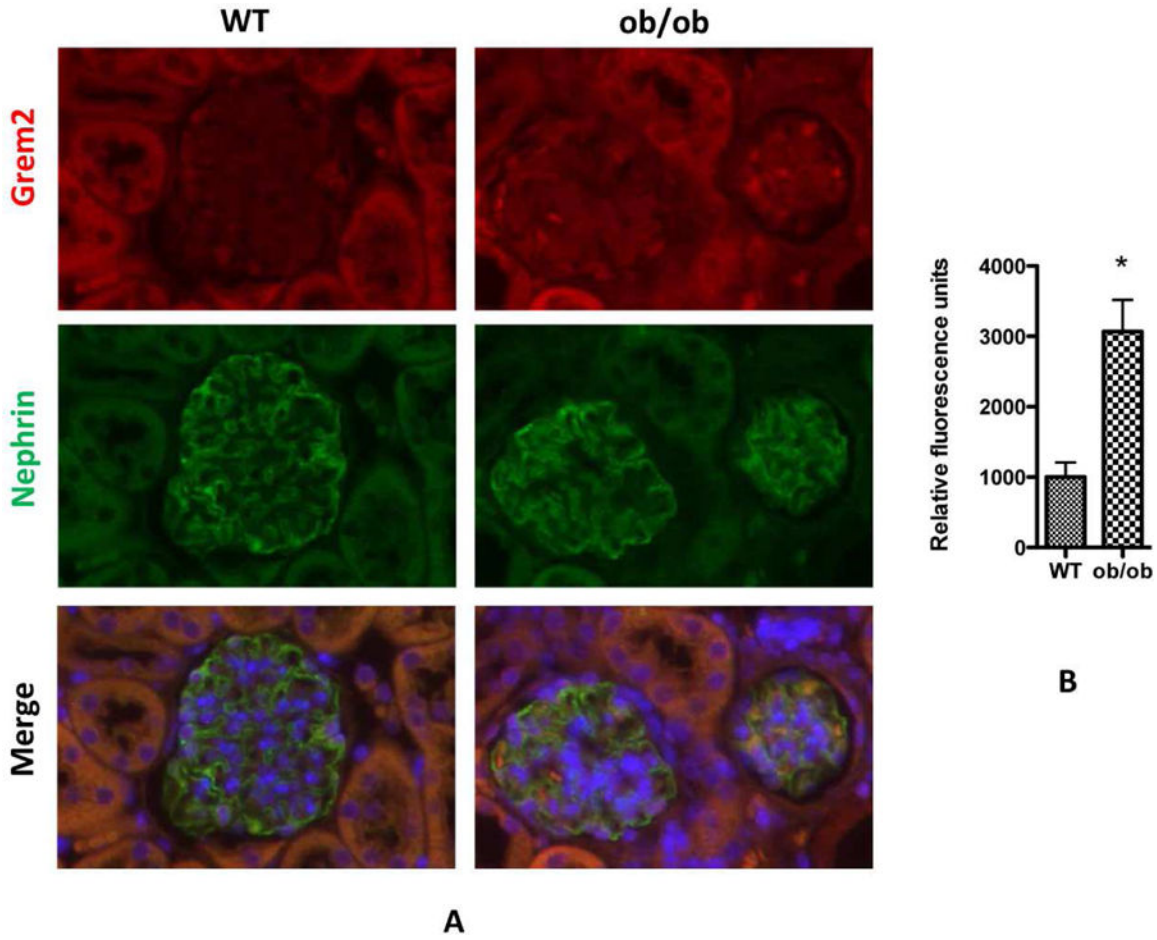

Figure 4. Expression of Grem2 in mouse glomeruli.

Paraffin sections were prepared from 14-week-old BTBR wild type (WT) and diabetic (ob/ob) mice for immunofluorescence staining to detect the Grem2 expression in the glomeruli. Nephrin was stained to display podocytes. Representative fluoromicrographs are displayed (A). The average fluorescence intensity was measured per region of interest (ROI) for Grem2, and the results (mean ± SD) represent 10 randomly selected regions (B). * $P < 0.05$ when compared with the wild type control mice.

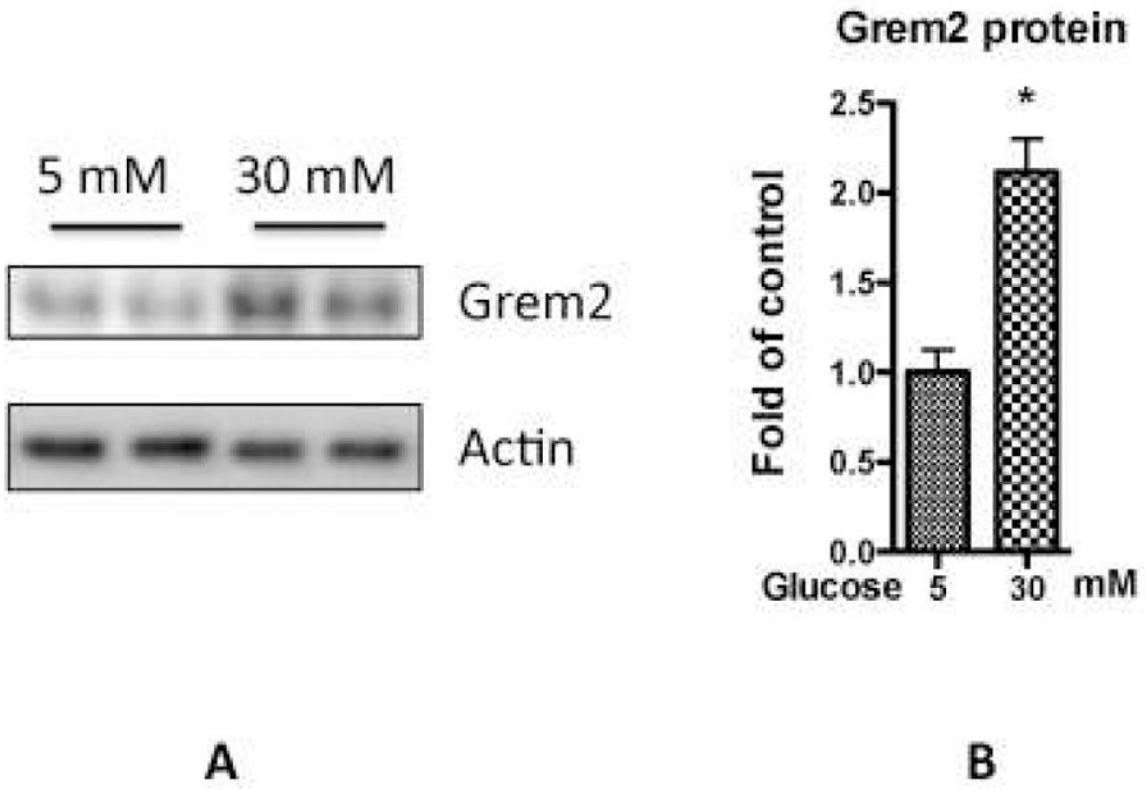

Figure 5. High glucose increases Grem2 expression in cultured human podocyte.

Human podocytes were cultured in media with normal (5 mM) and high (30 mM) glucose for 48 h. Cellular lysates were collected for the Western blotting assay to detect Grem2 protein expression. Representative gels are shown (A), and the protein bands were scanned, and the acquired images were analyzed using the public domain NIH image program for data quantification (B). Expression of Grem2 was normalized to β-actin, and the results (mean ± SD) represent three independent samples. $P < 0.05$ when compared with the treatment of 5 mM glucose.

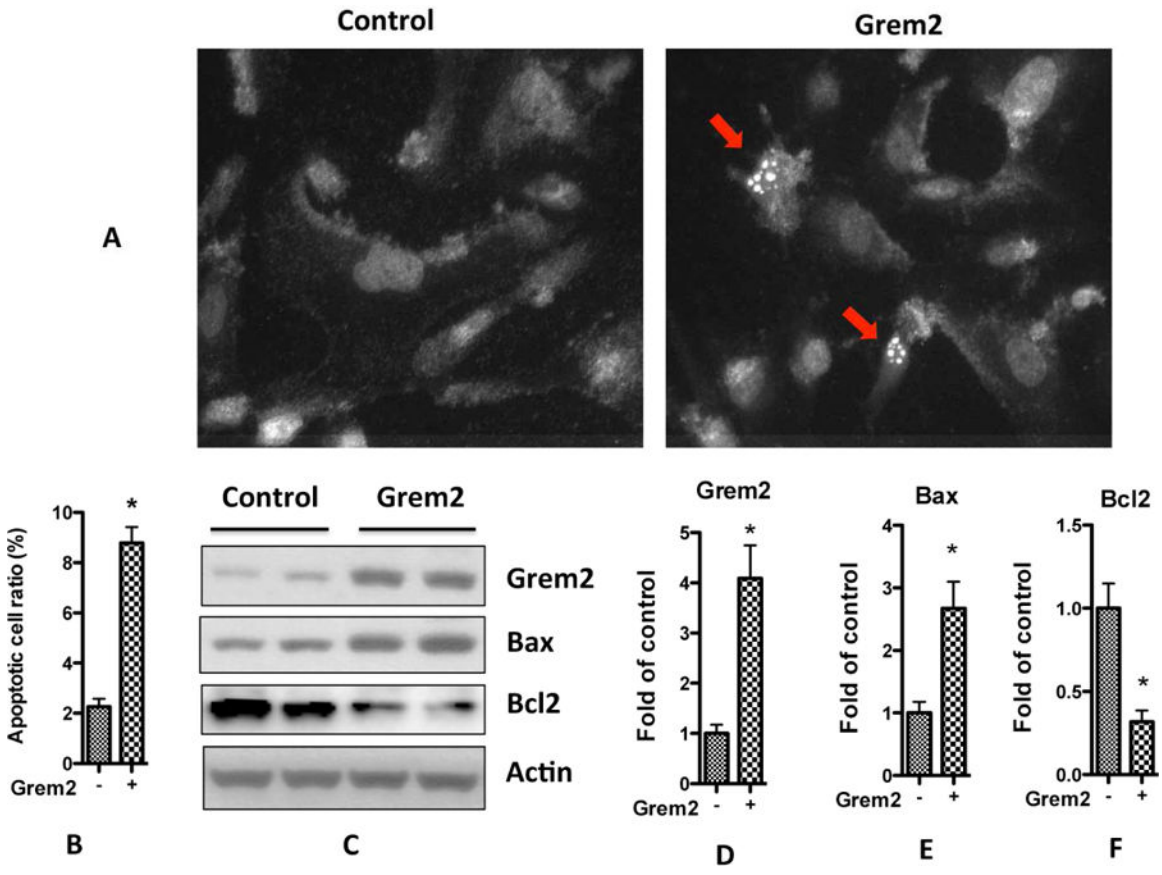

Figure 6. Overexpression of Grem2 increases podocyte apoptosis.

Human podocytes were transfected with Grem2 overexpression plasmid pCMV3-Grem2 and then were cultured in the medium for 48 h. A-B, apoptotic cells were examined and counted under microscope. Representative figures are displayed (A), and the results (mean ± SD) represent 10 randomly selected regions (B). C-F, cellular lysates were collected for Western blotting to detect the expression of apoptosis-related proteins, Bax and Bcl2. Representative gels are displayed (C). The protein bands were scanned, and the acquired images were analyzed using the public domain NIH image program for data quantification (D-F), and the results (mean ± SD) represent three independent samples. * $P < 0.05$ when compared with empty vector control.

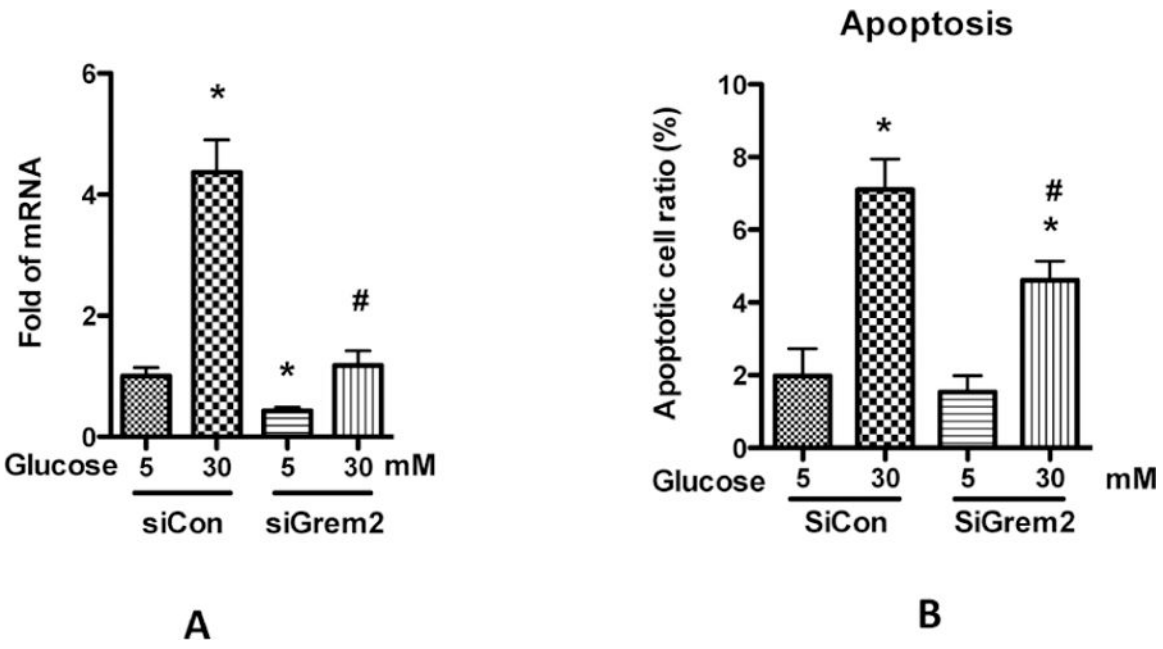

Figure 7. Silencing Grem2 partially attenuates high glucose-induced apoptosis.

Human podocytes were cultured in media with 5 or 30 mM glucose, and siRNA for control (SiCon) or for Grem2 (SiGrem2) were added to the cells. After 48 h, total RNAs were extracted, and real- time PCR was performed to determine the silence of Grem2 (A). In parallel experiments, apoptotic cells were determined with Hoechst33342 staining and were counted under a microscope (B). The results (mean ± SD) represent three independent samples. * $P < 0.05$ when compared with SiCon-5 mM; while # $p < 0.05$ when compared with SiCon-30 mM.

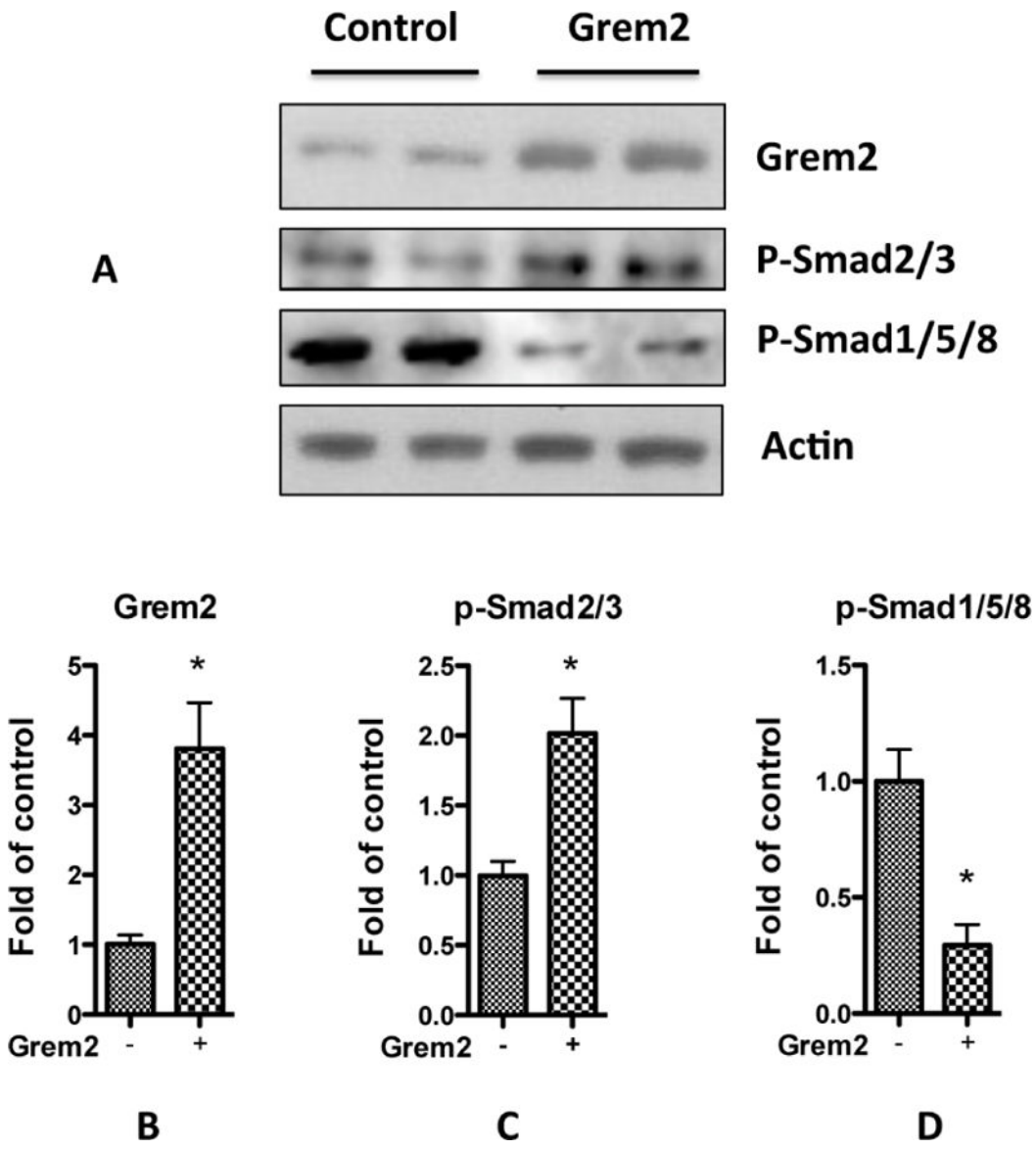

Figure 8. Overexpression of Grem2 affects the phosphorylation of Smads in cultured podocyte.

Human podocytes were transfected with/without Grem2 overexpression plasmid. After 48 h, the cellular lysates were collected and were subjected to Western blotting. Representative gels are shown (A), and the protein bands were scanned, and the acquired images were analyzed using the public domain NIH image program for data quantification (B-D). Expression of Grem2 (B), p-Smad2/3 (C), and p-Smad1/5/8 (D) was normalized to β-actin. The results (mean ± SD) represent three independent samples. * $P < 0.05$ when compared with control.

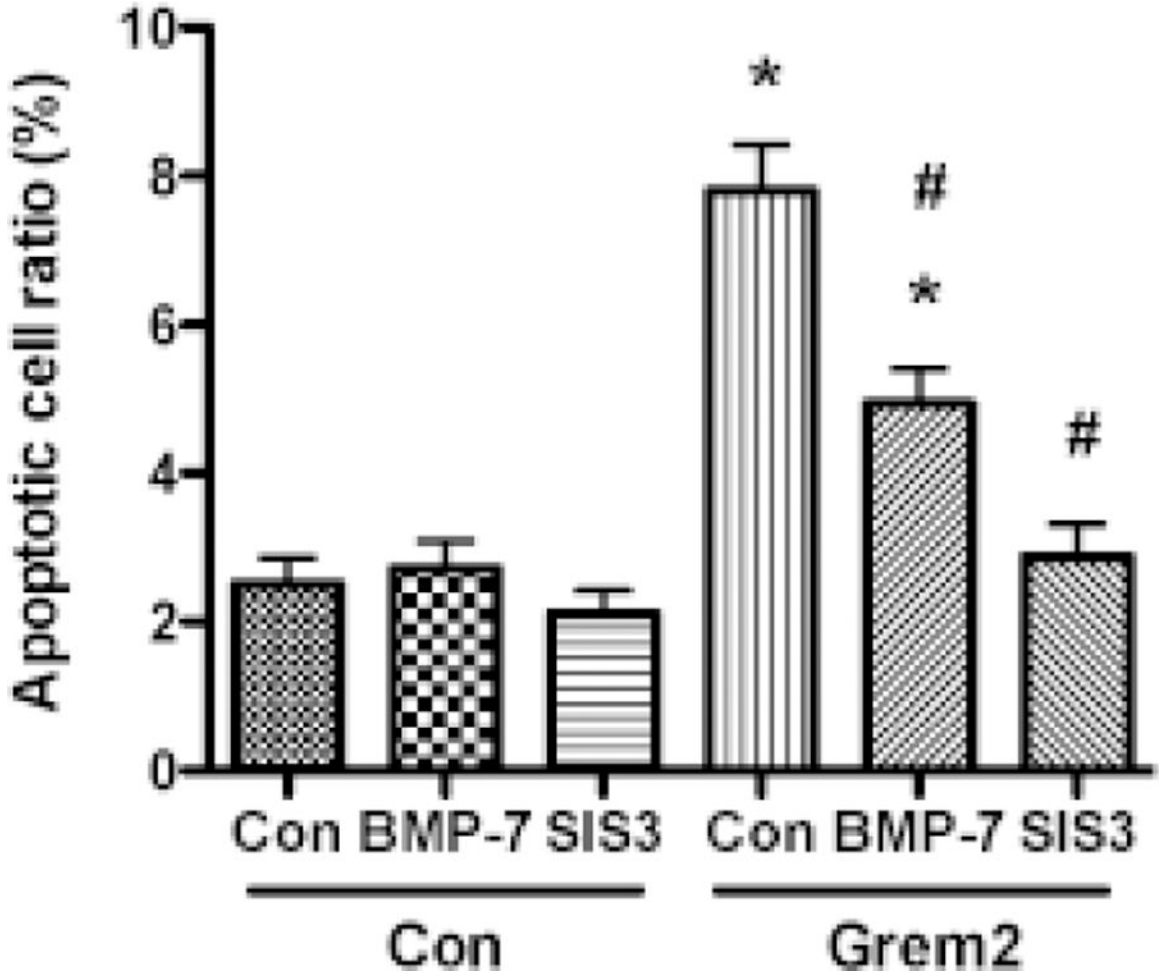

Figure 9. BMP-7 and SIS3 attenuate Grem2-induced podocyte apoptosis.

Human podocytes were transfected with/without Grem2 overexpression plasmid pCMV3-Grem2, and were then added with BMP-7 (100 ng/ml), an agonist for Smad1/5/8, or SIS3 (10 μM), an inhibitor for Smad2/3. After 48 h, the apoptotic cells were determined with Hoechst33342 staining and were counted under a microscope. The results (mean ± SD) represent 10 randomly selected pictures. * $P < 0.05$ when compared with control alone, while # $p < 0.05$ when compared with Grem2 overexpression alone.

Table 1.

Primers for real-time PCR

Gene	Forward primer	Reverse primer
Cer1	TGTGCCCTTCAACCAGACCAT	GTGGTGAATTTGGTGGGCGAG
Grem1	GCACATCCGAAAGGAGGAAG	ATGGATATGCAACGGCACTG
Grem2	GGAGGACTCCTTCCAATCCTG	TGTCGGAGTCACTCAGGTTCA
Grem3	CAGGGAGGAGGGCAGAGAGTAG	AGGCCTGGAGATCACCTGAACA
Nbl1	GCGTGCCTAGGACAATGCTTC	TCTACCAGCTTGTCCACCCTG
Sost	TTGGAGAGTACCCCGAGCCTC	CATGGGCCGTCTGTCAGGAAG
USAG1	TGGATCGGAGGAGGCTATGGA	GTTGTGGCTGGACTCGTTGTG